JOTCS B
Journal of the Turkish Chemical Society
Section: B
Chemical Engineering

TURKISH CHEMICAL SOCIETY

Removal of Lead and Cadmium Ions from Aqueous Solutions by Olive Pomace as a Low-Cost Biosorbent

Onur Uzunkavak, Günseli Özdemir*

Ege University, Faculty of Engineering, Chemical Engineering Department, Izmir, Turkey

Abstract: In this study, the adsorptive performance of olive pomace on lead and cadmium removal from aqueous solutions was investigated. Process parameters such as particle size, solution pH, contact time, initial ion concentration, and incubation temperature were evaluated using batch experiments. It was found that lead and cadmium adsorptions followed a pseudo second order kinetics. Sorption amount for lead and cadmium ions at 25 °C was obtained 33 and 8 mg/g, respectively, with 1 g/L olive pomace loading at pH 5.5 and 6. Adsorption isotherms were best fitted with the Redlich-Peterson and Langmuir-Freundlich models for lead and cadmium adsorptions, respectively. Thermodynamic calculations revealed that the adsorption process is feasible and spontaneous in nature. Adsorbent characterization was accomplished using ATR-FTIR, SEM, and BET analyses, whereas the surface charge was determined measuring the point of zero charge (pH_{PZC}).

Keywords: Wastewater treatment, biosorption, olive pomace, lead, cadmium.

Submitted: November 09, 2018. **Accepted:** April 16, 2019.

Cite this: Uzunkavak O, Özdemir G. Removal of Lead and Cadmium Ions from Aqueous Solutions by Olive Pomace as a Low-Cost Biosorbent. JOTCSB. 2019;2(2):121–32.

***Corresponding author.** E-mail: gunseli.ozdemir@ege.edu.tr.

INTRODUCTION

Environmental pollution problems have been a rising concern of modern engineering. Heavy metal pollution is one of the most serious problems and the removal of heavy metals from the environment is of particular importance since they are persistent and non-biodegradable (1,2). The most widely used methods developed for heavy metal removal include chemical or electrochemical precipitation, membrane filtration, ion exchange, evaporation, air stripping, steam stripping, and adsorption onto activated carbon (3,4). However, conventional methods are expensive and fail in heavy metal removal at low concentrations (5,6).

Biosorption is an attractive method which is advantageous over conventional techniques with the utilization of abundant and low-cost biomasses, namely biosorbents. It is also favored since it demonstrates superior metal binding capacities even at a low heavy metal ion concentration range of 1-100 ppm.

Lead and cadmium ions are not only non-essential to human body but also dangerous for human health. Lead poisoning causes neurodevelopmental problems in children, affects the membrane permeability of organs and haemoglobin synthesis. Lead is also a probable carcinogen because of its enzyme inhibitory effects (7). The presence of cadmium in humans may lead to osteoporosis and causes damages in kidneys (8). Lead-acid

batteries, ammunitions, paints, and ceramic products are major industrial applications of lead, whereas cadmium is mainly profited by the production of alloys, pigments, and batteries (9).

Olive pomace is an abundant agro-industrial waste of olive oil production in the Mediterranean region. There is no industrial use developed for olive pomace and it is normally incinerated or dumped without control. However, it is a promising biomaterial in wastewater treatment as a biosorbent. The utilization of olive pomace in biosorption of lead and cadmium ions is an effective, low-cost and environment-friendly activity adding value to this unrecognized waste (10,11).

The aim of this study was to present olive pomace as a proper biosorbent in lead and cadmium removal and show that it is applicable at its raw form implementing a greener operation without any further process in which chemicals are employed. Batch experiments were conducted and the optimum conditions for biosorption were identified evaluating the process parameters including particle size, solution pH, contact time, initial ion concentration, and incubation temperature. A kinetic modeling was performed in order to explain the adsorption mechanism. Adsorption isotherms were modeled to describe the equilibrium data and a thermodynamic study was carried out in order to have a better understanding of the adsorption characteristics of olive pomace at different temperatures. The surface properties of olive pomace was characterized using ATR-FTIR, SEM, and BET analyses, whereas the surface charge was determined measuring the point of zero charge (pH_{PZC}).

MATERIALS AND METHODS

All the chemicals and reagents used were of analytical grade. Deionized water was used for the preparation of solutions. The stock solutions of 100 ppm Pb^{2+} and 100 ppm Cd^{2+} were prepared from $Pb(NO_3)_2$ (Merck), and $Cd(NO_3)_2.4H_2O$ (Acros Organics), respectively. Their 10, 20, 40, 60, and 80 ppm solutions were prepared using serial dilution. HCl and NaOH used in pH adjustment were purchased from Merck. Olive pomace obtained from an olive oil plant was used in the biosorption experiments as a biosorbent.

Preparation of olive pomace

Olive pomace was thoroughly washed with tap, and deionized water and then dried at 50°C for 24 h. It was then milled and sieved using a Groschopp & Co mill and Tyler standard sieves. It was finally stored in airtight containers according to two size fraction ranges of 100-500 µm and 500-1000 µm for the further use.

Characterization of olive pomace

The attenuated total reflection-Fourier-transform infrared (ATR-FTIR) spectra of pristine, and loaded olive pomace (initial Pb^{2+} and Cd^{2+} of 100 ppm) were obtained in transition mode using a Perkin Elmer (Spectrum 100) spectrometer in the region 4000-400 cm^{-1}. The morphological features of olive pomace were observed using a Carl Zeiss (300VP) scanning electron microscope (SEM). The specific surface area of olive pomace was determined from the adsorption data of N_2 at 77 K using a BET analyzer (Micromeritics 3 Flex). Pb^{2+} and Cd^{2+} concentrations were specified using atomic absorption spectrometer (AAS) (Perkin Elmer AAnalyst 800).

Batch equilibrium method was applied to determine the point of zero charge (pH_{PZC}). Samples of 0.1 g of olive pomace were shaken in closed conical flasks with the addition of 50 mL of 0.01 M NaCl solution at 30°C. The pH was adjusted to a value between 2 and 12 with 0.1 M HCl or NaOH solutions using a pH meter (Hanna Instruments 221). The final pH was measured after 48 h of agitation. Then, the pH_{PZC} was determined at the point where the curve pH_{final} versus $pH_{initial}$ crosses the line $pH_{initial} = pH_{final}$ (12).

Adsorption experiments

Experiments were performed in 50 mL PP tubes with 0.025 g of olive pomace and 25 mL of Pb^{2+} or Cd^{2+} solutions of desired concentrations. Effect of particle size was investigated comparing the two size fraction ranges of 100-500 µm and 500-1000 µm in 24 h Pb^{2+} adsorption experiments with the initial Pb^{2+} concentrations of 10 to 100 ppm. Effect of solution pH was studied through 24 h of Pb^{2+} and Cd^{2+} adsorption experiments with the initial ion concentrations of 100 ppm and the pH variation of 2 to 10. Effect of contact time was observed in Pb^{2+} and Cd^{2+} adsorption experiments with the initial ion concentrations of 100 ppm at the optimum pH values varying the agitation time from 0.5 to 24 h. The effect of initial ion concentration was examined with the equilibrium adsorption experiments of Pb^{2+} and Cd^{2+} at the optimum pH values in the

initial ion concentration range of 10 to 100 ppm. Effect of incubation temperature on Pb^{2+} and Cd^{2+} adsorption was investigated at the optimum pH values in the initial ion concentration range of 10 to 100 ppm at 25, 35 and 45°C. All experiments were performed in duplicate. The supernatant liquids were filtered and analyzed using AAS to specify the resulting ion concentrations. The amount of Pb^{2+} and Cd^{2+} adsorbed was calculated as follows:

$$q_{eq}=\frac{(C_o-C_{eq})V}{m} \qquad \text{(Eq. 1)}$$

where q_{eq} is the equilibrium sorption (mg/g), C_o and C_{eq} are the initial and equilibrium ion concentrations (mg/L), V is the volume of solution (L), m is the amount of olive pomace (g).

Kinetic models

Kinetic models of "pseudo first order" (13), "pseudo second order" (14), "Weber-Morris intraparticle diffusion" (15), "Elovich" (16), "Bangham pore diffusion" (17), and "Boyd film diffusion" (18) were applied to explain the adsorption mechanism. The respective equations are expressed below:

$$\log(q_{eq}-q_t)=\log q_{eq}-K_1 \qquad \text{(Eq. 2)}$$

$$\frac{t}{q_t}=\frac{1}{K_2 q_{eq}^2}+\frac{t}{q_{eq}} \qquad \text{(Eq. 3)}$$

$$q_t=K_{diff}t^{0.5}+I \qquad \text{(Eq. 4)}$$

$$q_t=\frac{1}{\beta}\ln(\alpha\beta)+\frac{1}{\beta}\ln(t) \qquad \text{(Eq. 5)}$$

$$\log\left(\frac{C_0}{C_0-q_t m}\right)=\log\left(\frac{k_0 m}{2.303V}\right)+\alpha\log(t) \qquad \text{(Eq. 6)}$$

$$\ln\left(1-\frac{q_t}{q_{eq}}\right)=R^1 t \qquad \text{(Eq. 7)}$$

where q_{eq} and q_t are the amount of Pb^{2+} and Cd^{2+} adsorbed at equilibrium and at time t onto olive pomace (mg/g), respectively, K_1 is the rate constant of the pseudo first order model (L/min), K_2 is the rate constant of pseudo second order model (g/(mg.min)), K_{diff} is the intraparticle diffusion rate constant (mg/(g.$h^{0.5}$)), the value of I is the boundary layer thickness (mg/g), α is the initial adsorption rate (mg/(g.min)), β is the adsorption constant (g/mg), C_o is the initial ion concentration (mg/L), V is the volume of solution (mL), m is the amount of olive pomace (g/L), k_o is equilibrium constant, and R^1 is liquid film diffusion constant (1/min).

Isotherm models

Three 2-parameter isotherm models of "Langmuir", "Freundlich" and "Dubinin-Radushkevich", and three 3-parameter isotherm models of "Langmuir-Freundlich", "Radke-Prausnitz" and "Redlich-Peterson" were applied to describe the equilibrium data (19). The respective equations are expressed below:

$$q_{eq}=\frac{q_m K_L C_{eq}}{1+K_L C_{eq}} \qquad \text{(Eq. 8)}$$

$$q_{eq}=K_F C_{eq}^{1/n} \qquad \text{(Eq. 9)}$$

$$q_{eq}=(q_m)\exp(-K_{D-R}\epsilon^2) \qquad \text{(Eq. 10)}$$

$$q_{eq}=\frac{q_m(K_{L-F}C_{eq})^{m_{L-F}}}{1+(K_{L-F}C_{eq})^{m_{L-F}}} \qquad \text{(Eq. 11)}$$

$$q_{eq}=\frac{q_m K_{R-Pr} C_{eq}}{(1+K_{R-Pr}C_{eq})^{m_{R-Pr}}} \qquad \text{(Eq. 12)}$$

$$q_{eq}=\frac{K_{R-Pe}C_{eq}}{1+\alpha_{R-Pe}(C_{eq})^{\beta_{R-Pe}}} \qquad \text{(Eq. 13)}$$

where q_m is the monolayer capacity of olive pomace covered with Pb^{2+} and Cd^{2+} (mg/g), K_L is the Langmuir constant (L/mg) related to the energy of adsorption, K_F is the Freundlich constant which predicts the ion amount per gram olive pomace at equilibrium concentration ($mg^{(1-1/n)}.L^{1/n}/g$), n is a strength measure of the process and related to surface heterogeneity. Dubinin-Radushkevich (D-R) model has K_{D-R} as D-R isotherm constant (mol^2/kJ^2) and $\epsilon=RT\ln\left(1+\frac{1}{C_{eq}}\right)$, where R= 8.314 (J/mol.K) and T in Kelvin. The Langmuir-Freundlich constant, K_{L-F}, is related to the energy of adsorption and m_{L-F} values close to zero indicate heterogeneous sorbent, while values closer to unity indicate relatively homogeneous distribution of binding sites. The isotherm constants of Radke-Prausnitz (K_{R-Pr})

and Redlich-Peterson ($K_{R\text{-}Pe}$ and $\alpha_{R\text{-}Pe}$), as well as $m_{R\text{-}Pr}$ and $\beta_{R\text{-}Pe}$ have similar meanings as explained for Langmuir-Freundlich model (20,21).

Non-linear regression analyses of average relative error (ARE) and root mean square error (RMSE) for the isotherm models were applied using the respective equations below:

$$ARE = \frac{1}{n}\sum_{i=1}^{n}\left|\frac{q_{exp}-q_{calc}}{q_{exp}}\right|100 \quad \text{(Eq. 14)}$$

$$RMSE = \sqrt{\frac{\sum_{i=1}^{n}\left(q_{exp}-q_{calc}\right)^2}{n}} \quad \text{(Eq. 15)}$$

where n is the number of experimental data and q_{exp} and q_{calc} stand for the experimental and calculated sorption values (22). A smaller value of ARE and RMSE implies a better modeling.

Thermodynamic calculations

Thermodynamic parameters were calculated to reveal the thermal properties of olive pomace combining the equations below (23):

$$\Delta G^0 = -RT\ln K_D \quad \text{(Eq. 16)}$$

$$K_D = 1000\,K_F \quad \text{(Eq. 17)}$$

$$\Delta G^0 = \Delta H^0 - T\Delta S^0 \quad \text{(Eq. 18)}$$

where ΔG° is the standard free energy change, R is the universal gas constant, T is the absolute temperature in Kelvin, K_D is the distribution coefficient derived from K_F value of Freundlich isotherm model, ΔH° is the enthalpy change, and ΔS° is the entropy change. Van't Hoff equation finally yields as:

$$\ln K_D = -\frac{\Delta G^0}{RT} = -\frac{\Delta H^0}{RT} + \frac{\Delta S^0}{R} \quad \text{(Eq. 19)}$$

RESULTS AND DISCUSSION

Characterization of olive pomace

The point of zero charge (pH_{PZC}) measurement (Figure 1) revealed that the surface of olive pomace is neutral at pH 6.2, acidic (positively charged) below and basic (negatively charged) above this value which is capable of Pb^{2+} and Cd^{2+} adsorption. This property determines how easily heavy metal ions are captured on the surface of a biosorbent depending on the pH of the environment and the charge of the ions.

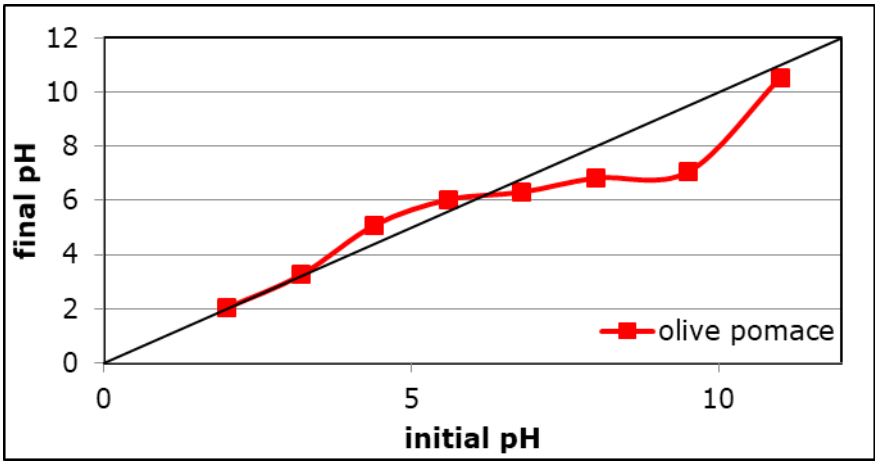

Figure 1. Plot of final pH vs. initial pH for point of zero charge measurement.

The BET surface area of olive pomace was determined as around 0.15 m^2/g using the BET analyzer. The small surface area indicated that the surface has a non-porous character. SEM analysis (Figure 2) also confirmed this non-porous structure illustrated with a magnification of 500x. Despite not having a large surface area, olive pomace was capable of Pb^{2+} and Cd^{2+} uptake.

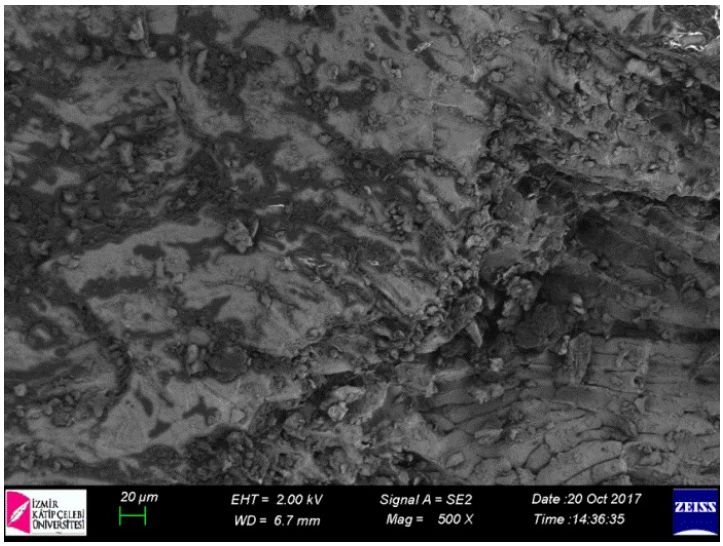

Figure 2. SEM micrograph of olive pomace with a magnification of 500x.

Surface functional groups of the pristine and Pb^{2+}/Cd^{2+} adsorbed olive pomace were analyzed using ATR-FTIR spectroscopy (Figure 3) to understand the nature of the surface functional groups and their interactions with Pb^{2+} and Cd^{2+} ions. The strong broad band at 3334 cm^{-1} is the characteristic peak ascribed to the -OH stretching vibrations. The peaks at 2923 and 2855 cm^{-1} are due to the C-H stretching vibrations of CH, CH_2 and CH_3 groups (10). The peak around 1724 cm^{-1} shows the carbonyl (C=O) stretching vibration of the carboxyl groups and the peak at 1655 cm^{-1} are initiated by the asymmetric stretching vibrations of the carboxylic groups (24). The peaks in the range of 1000 to 1300 cm^{-1} are generally ascribed to the C-O stretching vibrations in carboxylic acids and alcohols (25). The shifts on the peak locations from 3334, 1724 cm^{-1} to 3328, 1730 cm^{-1} after Pb^{2+} adsorption and to 3313, 1718 cm^{-1} after Cd^{2+} adsorption indicate the interactions with the related surface functional groups. It can be concluded from these results that the main groups (-OH and -COO) are promoting the Pb^{2+} and Cd^{2+} adsorption. Besides, the peak shifts from 2993 and 2855 cm^{-1} to the single peak at 2877 cm^{-1} after Cd^{2+} adsorption point out coordinative interaction of Cd^{2+} ions with the CH groups of the olive pomace surface. The largest peak shift identified for C-H stretching and the minor signal attenuation corresponding to CH_2 wagging was attributed to steric strain introduced by accommodation of the Cd^{2+} ions in coordination complex formation (26).

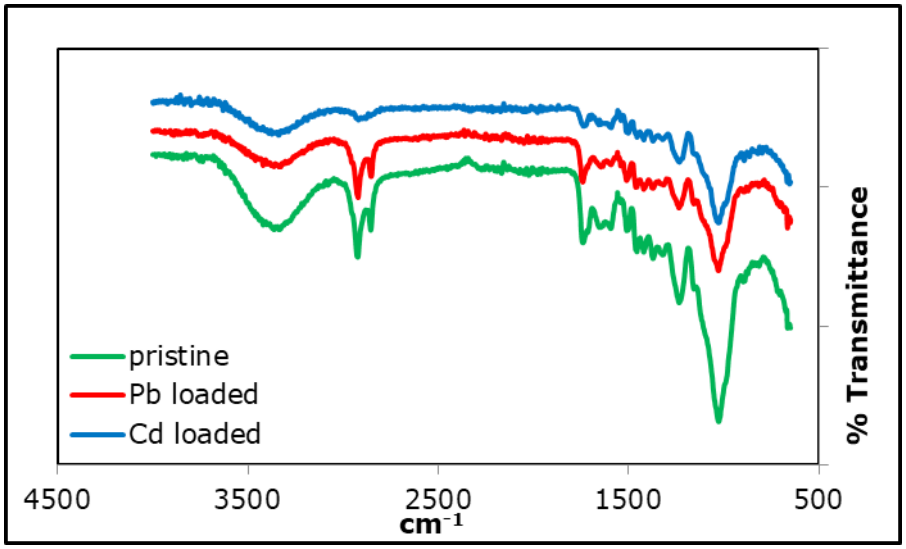

Figure 3. ATR-FTIR spectra of pristine, and Pb^{2+}/Cd^{2+} loaded olive pomace.

Effect of particle size

Effect of particle size was studied to choose a particle size with a higher uptake capacity. The results (Figure 4) revealed the insignificant difference between sorption capacities of the two size fraction ranges. Taking into account of the inevitable pressure drop created by finer solids in continuously operated systems, olive pomace fraction in the range of 500-1000 µm was utilized throughout the study to exhibit its ease of use in such potential technologies.

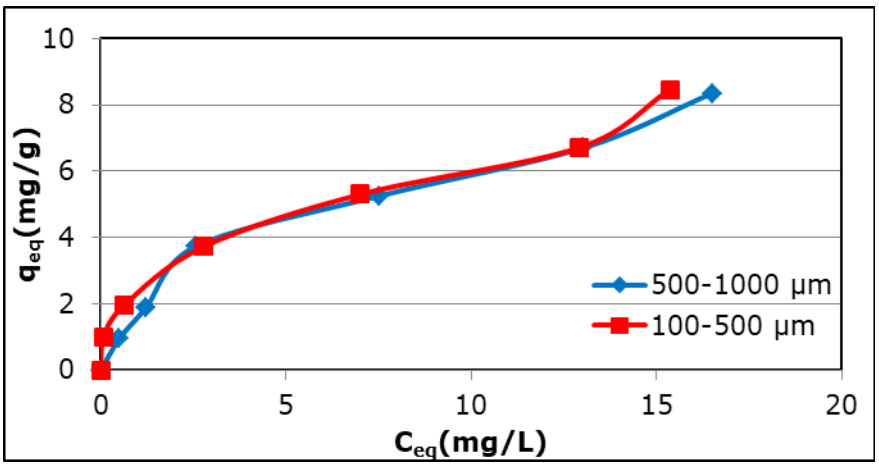

Figure 4. Plot of q_{eq} vs. C_{eq} for Pb^{2+} adsorption with different size fraction ranges.

Effect of solution pH

To study the pH dependency of the adsorption process, experiments were carried out at the pH range of 2-10. Solution pH affects not only the surface charge of the olive pomace but also the hydrolysis accompanying the precipitation of metal hydroxides. Metal hydroxides are amphoteric, that is, they are increasingly soluble at both low and high pH values, and the point of minimum solubility (optimum pH for precipitation) emerges at a pH different for each metal ion. According to Figure 5, the true adsorption of Pb^{2+} occurs until pH 6 and that of Cd^{2+} occurs until pH 7, whereas the formation of $Pb(OH)^{+}$ and $Cd(OH)^{+}$ ions begins at a pH higher than 6 and 7 for Pb^{2+} and Cd^{2+}, respectively. The figure further shows that no adsorption occurs due to the reduced attraction by the less negative surface charge and competing H^{+} ions at a pH

lower than 2 for Pb^{2+} and 3 for Cd^{2+} (27). Therefore, the optimum pH values were selected as 5.5 and 6 for Pb^{2+} and Cd^{2+}, respectively.

At the optimum pH conditions lower than the pH_{PZC} of 6.2, the adsorption is expected to take place by means of the ion exchange of Pb^{2+} and Cd^{2+} with H^+, as well as with Na^+ ions present on the surface.

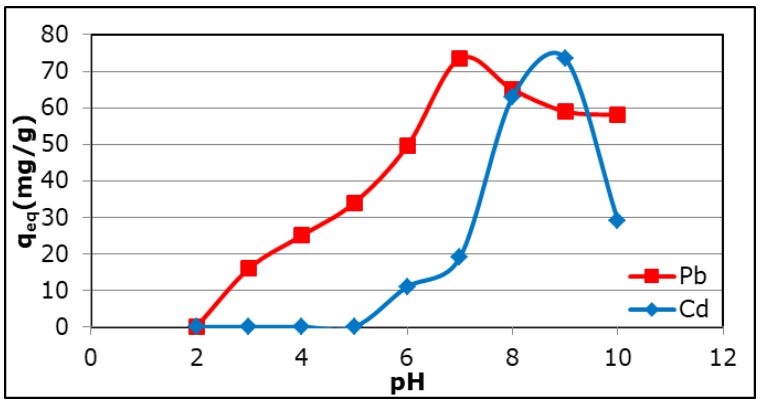

Figure 5. Plot of q_{eq} vs. pH for $Pb^{2+}$and Cd^{2+}adsorption.

Effect of contact time

Effect of contact time on Pb^{2+} and Cd^{2+} adsorption was studied to verify the sorption equilibrium. As seen in Figure 6, both Pb^{2+} and Cd^{2+} adsorption onto olive pomace are fast during the first four hours and then the equilibrium is attained slowly.

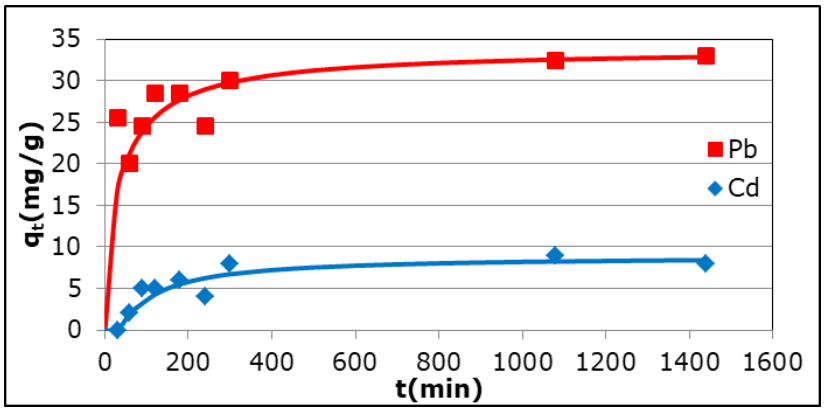

Figure 6. Plot of q_t vs. time with the pseudo second order model fitting for Pb^{2+} and Cd^{2+} adsorption.

Effect of initial ion concentration

Maximum sorption for Pb^{2+} and Cd^{2+} was obtained in the effect of initial ion concentration experiments at 25°C as 33 and 8 mg/g, respectively. The supremacy acquired by Pb^{2+} proves that the affinity of olive pomace towards Pb^{2+} is greater than that towards Cd^{2+}. Hence, a selective removal might be carried out from a bimetallic mixture of these ions.

Effect of incubation temperature

A direct proportion between the sorption capacity and incubation temperature for both Pb^{2+} and Cd^{2+} was indicated by the effect of incubation temperature experiments. This behavior is exhibited in Figure 7 with the best fitting isotherm models which are the Redlich-Peterson and Langmuir-Freundlich models for Pb^{2+} and Cd^{2+} adsorption, respectively. The modeling study is discussed further in the isotherm modeling section.

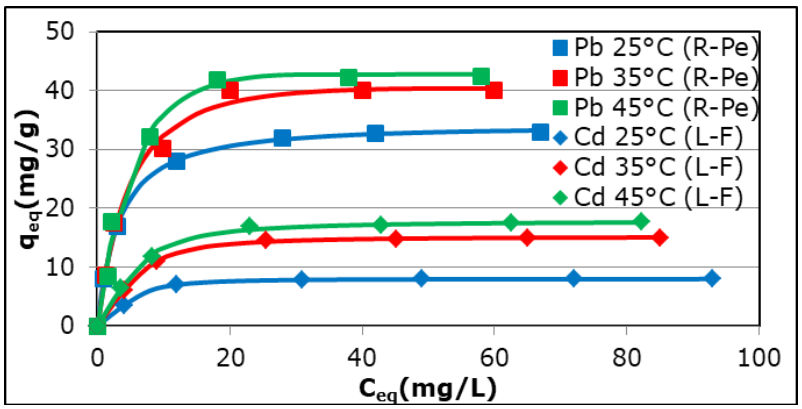

Figure 7. Plot of q_{eq} vs. C_{eq} for Pb^{2+} and Cd^{2+} adsorption at different temperatures.

Kinetic modeling

Linear plots of the pseudo first order (P-F-O), pseudo second order (P-S-O), Weber-Morris intraparticle diffusion, Elovich, Bangham pore diffusion, and Boyd film diffusion models were applied and compared. Based on the coefficient of determination (R^2) values close to unity given in Table 1 and the graphical harmony seen in Figure 8, pseudo second order model is the most suitable kinetic model for both Pb^{2+} and Cd^{2+} adsorption. Since pseudo second order model originates from chemical reaction kinetics, the three consecutive steps of adsorption, namely bulk diffusion, film diffusion and pore diffusion are not addressed in the rate-limiting step determination. In this regard, Weber-Morris intraparticle diffusion model is useful to find out the rate-limiting step. As seen in Figure 8c, there are two linear portions: The first controlled by surface diffusion process, and the latter by pore diffusion, indicating that external diffusion is the rate-limiting step (17,18).

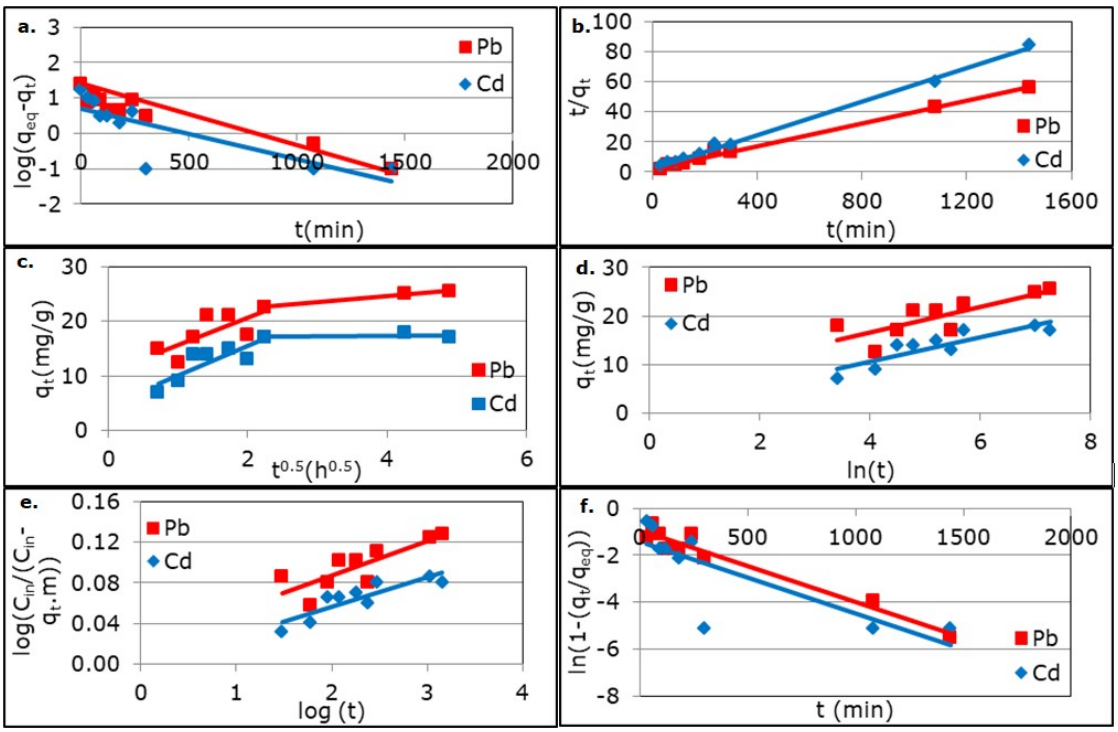

Figure 8. Kinetic models of a) P-F-O, b) P-S-O, c) Weber-Morris, d) Elovich, e) Bangham, and f) Boyd.

Table 1. Kinetic parameters for Pb^{2+} and Cd^{2+} adsorption.

Kinetic model	parameter	Pb^{2+}	Cd^{2+}
P-F-O	K_1 (L/min)	0.0017	0.002
	q_{eq} (mg/g)	25.119	16.596
	R^2	0.774	0.412
P-S-O	K_2 (g/(mg.min))	0.0007	0.0013
	q_{eq} (mg/g)	26.316	17.921
	R^2	0.996	0.996
Weber-Morris	K_{diff} (mg/(g.$h^{0.5}$))	1.155	5.410
	I (mg/g)	19.954	4.743
	R^2	0.993	0.718
Elovich	α (mg/g.min)	24.441	2.929
	β (g/mg)	0.375	0.392
	R^2	0.646	0.764
Bangham	A	0.033	0.029
	k_o	60.344	57.271
	R^2	0.661	0.771
Boyd	R^1 (min^{-1})	0.003	0.003
	R^2	0.949	0.643

Isotherm modeling

Parameters of the isotherm models as well as their corresponding average relative errors (ARE) and root mean square errors (RMSE) were estimated using solver add-in function of Microsoft Excel. The best simulation was selected considering the graphical harmony of the equilibrium data with the models and also the lowest values of ARE and RMSE.

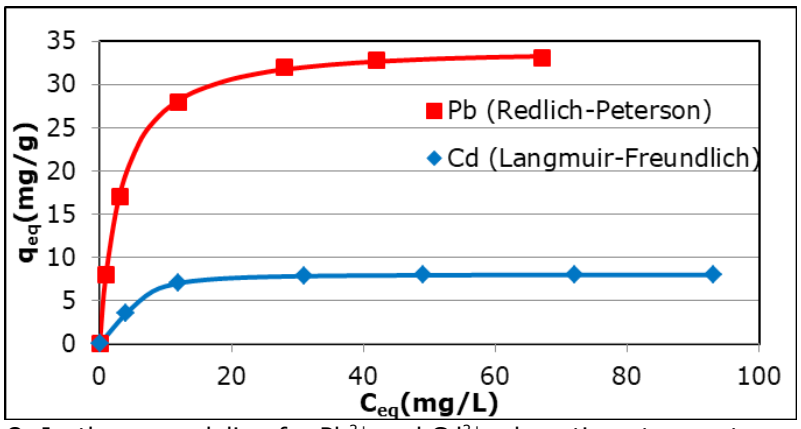

Figure 9. Isotherm modeling for Pb^{2+} and Cd^{2+} adsorption at room temperature.

Redlich-Peterson and Langmuir-Freundlich models were the best resulting models for Pb^{2+} and Cd^{2+} adsorption, respectively, as shown in Figure 9, and the parameters of these models are presented in Table 2 (see also Figure 7). The Redlich-Peterson model approximates the Henry's law at low Pb^{2+} concentrations, and at high concentrations it predicts a monolayer adsorption capacity characteristic of the Langmuir isotherm. On the other hand, the

Langmuir-Freundlich model reduces to the Freundlich isotherm at low Cd^{2+} concentrations, while it behaves like the Langmuir isotherm at high concentrations. The m and β parameters are often regarded as the heterogeneity factors and the calculated values (Table 2) greater than unity confirms the heterogeneous nature of the olive pomace. (19,20,21). The steep slope observed for Pb^{2+} adsorption proves that olive pomace is very effective in the removal of this ion at low concentrations, whereas Cd^{2+} adsorption appears to be less favorable. This behavior is in line with the best fitting models to the equilibrium data of Pb^{2+} and Cd^{2+} adsorption at low concentrations corresponding to the steep and linear portion for Henry's isotherm and the less steep portion for Freundlich isotherm, respectively.

Table 2. Isotherm parameters for Pb^{2+} and Cd^{2+} adsorption at different temperatures.

heavy metal ion	T (K)	isotherm model	q_m	K	m	α	β	ARE	RMSE
Pb^{2+}	298	Redlich-Peterson		10.69		0.28	1.02	0.46	0.24
	308			8.64		0.13	1.10	0.65	1.47
	318			8.00		0.08	1.19	1.68	1.88
Cd^{2+}	298	Langmuir-Freundlich	8.00	0.22	2.00			0.17	0.03
	308		15.00	0.20	1.76			0.04	0.09
	318		17.80	0.20	1.62			0.73	0.36

Thermodynamic parameters

Thermodynamic behavior of olive pomace was evaluated with the calculated thermodynamic parameters. The slope and intercept of the plot $\ln K_D$ vs. 1/T given in Figure 10 were used in the calculation of the enthalpy and entropy changes in Van't Hoff equation.

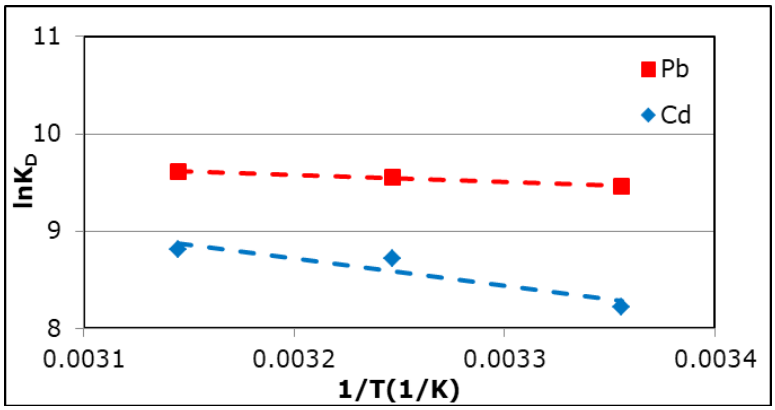

Figure 10. Plot of $\ln K_D$ vs. 1/T for Pb^{2+} and Cd^{2+} adsorption at different temperatures.

The negative values of ΔG° state that the adsorption phenomenon is feasible and spontaneous. The positive values of ΔH° denote an endothermic process, indicating the increased amount of metal ions adsorbed with the increase in temperature. The magnitude of ΔH° also gives an idea about the type of adsorption suggesting that Pb^{2+} and Cd^{2+} adsorption can be attributed to a physical adsorption process. Besides, the positive values of ΔS° indicates an increased disorder at the solid-solution interface reflecting the affinity of olive pomace towards Pb^{2+} and Cd^{2+}, and the adsorption mechanism based on the ion exchange (28).

Table 3. Thermodynamic parameters for Pb^{2+} and Cd^{2+} adsorption at different temperatures.

heavy metal ion	T (K)	K_D	$\ln K_D$	ΔG° (kJ/mol)	ΔH° (kJ/mol)	ΔS° (J/mol.K)
	298	12876.91	9.46	-23.446		
Pb^{2+}	308	14058.42	9.55	-24.457	6.018	98.896
	318	14999.36	9.62	-25.423		
	298	3721.43	8.22	-20.370		
Cd^{2+}	308	6124.18	8.72	-22.329	23.253	146.913
	318	6686.97	8.81	-23.287		

CONCLUSION

This study introduced olive pomace as a proper biosorbent in the removal of lead and cadmium ions from aqueous solutions. Its application at its raw form offers an economical practice. The feasible and spontaneous behavior of the process was verified by the thermodynamic calculations. The endothermic process indicated the increased metal uptake with an increase in temperature. The adsorption kinetics was well explained with the pseudo second order model. The Redlich-Peterson and Langmuir-Freundlich isotherms were the best fitting models for Pb^{2+} and Cd^{2+} adsorption, respectively. The Pb^{2+} amount adsorbed was four times higher than that of Cd^{2+}. The supremacy acquired by Pb^{2+} proves that the affinity of olive pomace towards Pb^{2+} is greater than that towards Cd^{2+}. Hence, a selective removal might also be carried out from a bimetallic mixture of these ions.

ACKNOWLEDGEMENTS

The authors are grateful to Ege University Research Fund for the financial support under Project No 14-MUH-052 and Van Yüzüncü Yıl University for holding the 13th National Chemical Engineering Congress (September 3-6, 2018) where this study was orally presented.

REFERENCES

1. Yakub A, Mughal MS, Mukhtar H, Spirogyra as an efficient biosorbent of cadmium: A mechanistic approach. Pakistan Journal of Botany. 2016; 48(6): 2563-70.

2. Lawal OS, Ayanda OS, Rabiu OO, Adebowale KO, Application of black walnut (Juglannigra) husk for the removal of lead (II) ion from aqueous solution. IWA Publishing. 2017; 1-10.

3. Verma A, Kumar S, Kumar S, Biosorption of lead ions from the aqueous solution by Sargassumfilipendula: Equilibrium and kinetic studies. Journal of Environmental Chemical Engineering. 2016; 4: 4587-99.

4. Husein DZ, Aazam E, Battia M, Adsorption of cadmium (II) onto watermelon rind under microwave radiation and application into surface water from Jeddah, Saudi Arabia. Arabian Journal for Science and Engineering. 2017; 42: 2403-15.

5. Mohammed A, Biosorption of lead, cadmium, and zinc onto sunflower shell: Equilibrium, kinetic, and thermodynamic studies. Iraqi Journal of Chemical and Petroleum Engineering. 2015; 16(1); 91-105.

6. Liu X, Chen ZQ, Han B, Su CL, Han Q, Chen, WZ, Biosorption of copper ions from aqueous solution using rape straw powders: Optimization, equilibrium and kinetic studies. Ecotoxicology and Environmental Safety. 2018; 150: 251-9.

7. Morosanu I, Teodosiu C, Paduraru C, Ibanescu D, Tofan, L, Biosorption of lead ions from aqueous effluents by rapeseed biomass. New Biotechnology. 2017; 39: 110-24.

8. Nishikawa E, da Silva MGC, Vieira MGA, Cadmium biosorption by alginate extraction waste and process overview in life cycle assessment context. Journal of Cleaner Production. 2018; 178: 166-75.

9. Tchounwou PB, Yedjou CG, Patlolla AK, Sutton DJ, Heavy Metals Toxicity and the Environment. EXS. 2012; 101: 133-64.

10. Martin-Lara MA, Pagnanelli F, Mainelli S, Calero M, Toro L, Chemical treatment of olive pomace: Effect on acid-basic properties and metal

biosorption capacity. Journal of Hazardous Materials. 2008; 156(1-3): 448-57.

11. Martin-Lara MA, Blazquez G, Ronda A, Perez A, Calero M, Development and characterization of biosorbents to remove heavy metals from aqueous solutions by chemical treatment of olive stone. Industrial & Engineering Chemistry Research. 2013; 52: 10809-19.

12. Shouman MA, Fathy NA, Khedr SA, Attia AA, Comparative biosorption studies of hexavalent chromium ion onto raw and modified palm branches. Advances in Physical Chemistry. 2013; 1-9.

13. Lagergren S, About the Theory of so Called Adsorption of Soluble Substances. Kungliga Svenska Vetenskapsakademiens Handlingar. 1898; 24: 1-39.

14. Febrianto J, Kosasih AN, Sunarso J, Ju YH, Indraswati N, Ismadji S, Equilibrium and kinetic studies in adsorption of heavy metals using biosorbent: A summary of recent studies. Journal of Hazardous Materials. 2009; 162: 616-45.

15. Weber JW, Morris JC, Kinetics of adsorption on carbon from solution. Journal of the Sanitary Engineering Division. 1963; 89: 31-60.

16. Hashem A, Adam E, Hussein HA, Sanousy MA, Ayoub A, Bioadsorption of Cd (II) from contaminated water on treated sawdust: Adsorption mechanism and optimization. Journal of Water Resource and Protection. 2013; 5: 82-90.

17. Chakrapani C, Babu CS, Vani KNK, Rao KS, Adsorption kinetics for the removal of fluoride from aqueous solution by activated carbon adsorbents derived from the peels of selected citrus fruits. E-Journal of Chemistry. 2010; 7(1): 419-27.

18. Qiu H, Pan B-C, Zhang Q-J, Zhang W-M, Zhang Q-X, Critical review in adsorption kinetic models. Journal of Zhejiang University SCIENCE A. 2009; 10(5): 716-24.

19. Foo KY, Hameed BH, Insights into the modeling of adsorption isotherm systems. Chemical Engineering Journal. 2010; 156: 2-10.

20. Montazer-Rahmati MM, Rabbani P, Abdolali, A, Keshtkar AR, Kinetics and equilibrium studies on biosorption of cadmium, lead, and nickel ions from aqueous solutions by intact and chemically modified brown algae. Journal of Hazardous Materials. 2011; 185: 401-407.

21. Saadi R, Saadi Z, Fazaeli R, Fard NE, Monolayer and multilayer adsorption isotherm models for sorption from aqueous media. Korean Journal of Chemical Engineering. 2015; 32(5): 787-799.

22. Ghaffari HR, Pasalari H, Tajvar A, Dindarloo K, Goudarzi B, Alipour V, Ghanbarneajd A, Linear and nonlinear two-parameter adsorption isotherm modeling: A case-study. The International Journal of Engineering and Science. 2017; 6(9): 1-11.

23. Tran HN, You SJ, Hosseini-Bandegharaei A, Chao HP, Mistakes and inconsistencies regarding adsorption of contaminants from aqueous solutions: A critical review. Water Research. 2017; 120: 88-116.

24. Almasi A, Omidi M, Khodadadian M, Khamutian R, Gholivand MB, Lead(II) and cadmium(II) removal from aqueous solution using processed walnut shell: Kinetic and equilibrium study. Toxicological & Environmental Chemistry. 2012; 94(4): 660-671.

25. Feng N, Guo X, Liang S, Adsorption study of copper (II) by chemically modified orange peel. Journal of Hazardous Materials. 2009; 164(2-3): 1286-1292.

26. Moyo M, Pakade VE, Modise SJ, Biosorption of lead(II) by chemically modified Mangiferaindica seed shells: Adsorbent preparation, characterization and performance assessment. Process Safety and Environmental Protection. 2017; 111: 40-51.

27. Pehlivan E, Yanik BH, Ahmetli G, Pehlivan M, Equilibrium isotherm studies for the uptake of cadmium and lead ions onto sugar beet pulp. Bioresource Technology. 2008; 99(9): 3520-3527.

28. Tadashi M, editor. Thermodynamics. Chapter 16: Insight Into Adsorption Thermodynamics, InTech; 2011.